Molecular Vision 2020; 26:691-704 <http://www.molvis.org/molvis/v26/691>
Received 14 October 2019 | Accepted 8 October 2020 | Published 10 October 2020

Neuroprotective effects of Acer palmatum thumb. leaf extract (KIOM-2015E) against ischemia/reperfusion-induced injury in the rat retina

Yeoun-Hee Kim,[1] Tae Woo Oh,[2] Eunhee Park,[3] Nam-Hui Yim,[2] Won-Kyung Cho,[2] Jin-Yeul Ma[2]

[1]Mirae Biopharm, Sagimakgol-ro, Jungwon-gu, Seongnam-si, Gyeonggi-do, Republic of Korea; [2]Korean Medicine (KM)-Application Center, Korea Institute of Oriental Medicine (KIOM), Cheomdan-ro Dong-gu, Daegu, South Korea; [3]Korean Drug CO.,LTD., Gil, Nonhyeon-Ro, Gangnam-Gu, Seoul, Republic of Korea

Purpose: The present study aimed to determine whether the administration of Acer palmatum thumb. leaf extract (KIOM-2015E) protects against the degeneration of rat retinal ganglion cells after ischemia/reperfusion (I/R) induced by midbrain cerebral artery occlusion (MCAO).

Methods: Sprague–Dawley rats were subjected to 90 min of MCAO, which produces transient ischemia in both the retina and brain due to the use of an intraluminal filament that blocks the ophthalmic and middle cerebral arteries. This was followed by reperfusion under anesthesia with isoflurane. The day after surgery, the eyes were treated three times (eye drop) or one time (oral administration) daily with KIOM-2015E for five days. Retinal histology was assessed in flat mounts and vertical sections to determine the effect of KIOM-2015E on I/R injury.

Results: A significant loss of brain-specific homeobox/POU domain protein 3A (Brn3a) and neuron-specific class III beta-tubulin (Tuj-1) fluorescence and a marked increase in glial fibrillary acidic protein (GFAP) and glutamine synthetase (GS) expression were observed after five days in the PBS-treated MCAO group compared to the sham-operated control group. However, KIOM-2015E treatment reduced (1) MCAO-induced upregulation of GFAP and GS, (2) retinal ganglion cell loss, (3) nerve fiber degeneration, and (4) the number of TUNEL-positive cells. KIOM-2015E application also increased staining for parvalbumin (a marker of horizontal cell associated calcium-binding protein and amacrine cells) and recoverin (a marker of photoreceptor expression) in rats subjected to MCAO-induced retinal damage.

Conclusions: Our findings indicated that KIOM-2015E treatment exerted protective effects against retinal damage following MCAO injury and that this extract may aid in the development of novel therapeutic strategies for retinal diseases, such as glaucoma and age-related macular disease.

Retinal ischemia, often referred to as "stroke of the retina," is an important cause of visual impairment in patients with retinal vascular occlusion, diabetic retinopathy, glaucoma, and ocular trauma [1-5]. The death of retinal ganglion cells (RGCs) is caused by a variety of mechanisms following ischemia/reperfusion (I/R) injury, including necrosis, apoptosis, necroptosis, and autophagy [6-8]. Retinal damage caused by I/R injury is associated with loss of neurons, morphological degeneration of the retina, loss of retinal function, and ultimately loss of vision [9-11]. Although degeneration times vary under different experimental conditions, I/R-induced injury and retinal degeneration are initially observed primarily in the inner retinal layers (e.g., the inner plexiform layer (IPL) and inner nuclear layer (INL)), which are supplied by the central retinal artery. In contrast, the outer nuclear layer (ONL) is generally less affected [12-15]. This structural difference may influence the initiation of I/R injury.

Middle cerebral artery occlusion (MCAO) in rodents is one of the most common experimental paradigms for inducing focal cerebral ischemia [16-18]. Retinal ischemia induced by ligation or clamping of the ophthalmic artery is a reproducible model of central nervous system (CNS) stroke that is highly amenable to experimental manipulation [3,9]. Steele et al. reported that MCAO induces retinal ischemic damage because the ophthalmic artery originates from the internal carotid artery and is proximal to the origin of the middle cerebral artery (MCA) [19]. As the ophthalmic artery that provides the main supply to the inner retina originates from the internal carotid artery, occlusion of the MCA will simultaneously interrupt the vascular supply to the retina and the whole eye [20-22]. Previous studies have indeed demonstrated that MCAO results in retinal ischemia in rats [22-24]. Therefore, MCAO is a useful model for researchers who aim to understand the changes that lead to retinal damage in human patients [19,22] and may also aid in the development of novel therapeutic strategies for retinal ischemia.

Correspondence to: Jin Yeul Ma, Korean Medicine (KM)-Application Center, Korea Institute of Oriental Medicine (KIOM), 70, Cheomdan-ro Dong-gu, Daegu, 41062, South Korea; Phone: +82-53-940-3811; FAX: +82-53-940-3899; email: jyma@kiom.re.kr

KIOM-2015E is an extract of Acer palmatum Thumb. leaves. In this experiment, the hot water extract, KIOM-2015EW, and the ethanol extract, KIOM-2015EE, were used. Plants of the genus *Acer* (Aceraceae)—commonly known as maple—have been used extensively in the traditional treatment of various diseases in East Asia and North America [25]. Several research groups have investigated the biologic and pharmacological activities of these plants, which contain several phytochemicals and are known to possess antioxidant, anti-tumor, and anti-inflammatory properties [26-28]. Clinical studies have revealed that medicinal plants belonging to the *Acer* genus are highly effective in the treatment of rheumatism, bruises, hepatic disorders, eye disease, and pain and in detoxification [25]. Modern pharmacological studies have confirmed the traditional uses of these important *Acer* species. Arnason et al. reported the traditional use of several Acer plants by the native population of eastern Canada. For example, *A. saccharum* Marshall is used to treat shortness of breath, eye pain, and cataracts, while *A. rubrum* L. and *A spicatum* Lam. are used to alleviate soreness of the eye [29]. *A. tataricum* subsp. ginnala (Maxim.) Wesm., which has traditionally been used to reduce redness and swelling of the eyes, has further been observed to exhibit anti-inflammatory activity in vitro [25]. Recently, we demonstrated that KIOM-2015EW has anti-inflammatory and anti-apoptotic effects in a hyperosmolar stress-induced in vitro dry eye model [30].

Although plants of the *Acer* genus are widely used worldwide for medicinal purposes, until recently little research has been conducted regarding the use of these plants for the treatment of ocular disease. In the present study, we investigated the effect of the novel therapeutic agent KIOM-2015E—a natural extract obtained from *Acer palmatum* Thumb. leaves—in a rat model of MCAO-induced retinal ischemia injury. Our report is the first to describe the neuroprotective effect of KIOM-2015E in a rat model of retinal ischemic injury induced by MCAO.

METHODS

Reagents: Monoclonal anti-brain-specific homeobox/POU domain protein 3A (Brn3a) was purchased from Santa Cruz Biotechnology, Inc. (Santa Cruz, CA). Monoclonal anti-neuron-specific beta-III tubulin (Tuj-1) was obtained from R&D Systems (Minneapolis, MN). Polyclonal anti-glial fibrillary acidic protein (GFAP) was purchased from Dako (Carpenteria, CA). Monoclonal anti-protein kinase C alpha (PKCα) and polyclonal anti-glutamine synthetase (GS) were purchased from Thermo Fisher Scientific (Waltham, MA). Polyclonal anti-parvalbumin was obtained from Abcam (Cambridge, MA). Polyclonal anti-recoverin was purchased from Millipore (Belrica, MA). Mounting medium with DAPI was purchased from Vector Laboratories (Burlingame, CA).

Preparation of herbal extracts, KIOM-2015EW and KIOM-2015EE: Acer palmatum: Thumb. leaves were purchased from Korea Medicine Herbs Association (Yeongcheon, Korea), confirmed by Professor K_i Hwan Bae of the College of Pharmacy at Chungnam National University (Daejeon, Korea), and then stored in the herbal bank of the Korea Institute of Oriental Medicine (KIOM). To prepare KIOM-2015EW, dried Acer palmatum Thumb. leaves (1700 g) were ground into a fine powder, soaked in 17 L distilled water, and then heat-extracted in an extractor (Cosmos-600 Extractor, Gyeonseo Co., Inchon, Korea) for 3 h at 115 °C. To prepare KIOM-2015EE, the fine *Acer palmatum* Thumb. powder (1700 g) was soaked in 17 L of 25% ethanol and extracted in a shaking incubator at room temperature for 24 h. The KIOM-2015EE extract was filtered using standard testing sieves (150 µm, Retsch, Haan, Germany), following which it was concentrated to dryness in a lyophilizer. KIOM-2015EE powder (50 mg) dissolved in 1 ml of distilled water was filtered through a 0.22-µm disk filter and maintained at −20 °C before use.

Animals: Male Sprague–Dawley (SD) rats weighing 280±10 g (Orient Bio Inc., Gyeonggi-do, South Korea) were used for all experiments. The animals were housed under controlled environmental conditions in an ambient temperature of 23±1 °C and relative humidity of 50±10% under a 12-h light/dark cycle and were given ad libitum access to food and water. All animal experiments were approved by and performed in accordance with the guidelines of the Animal Care and Use Committee of KIOM (Daejeon, Korea; reference number: D-16–004).

MCAO-induced retinal ischemic injury in rats: MCAO was induced in accordance with standard procedures (Longa et al., 1989). Briefly, rats were anesthetized with 100% oxygen containing 3% isoflurane. Rectal temperature was measured using a rectal probe and maintained at 37 °C with a heating pad (FHC Inc., Bowdoin ME) during the surgical procedure. The left common carotid artery was exposed, carefully separated from the vagus nerve, and ligated at the more proximal side via a right paramedian incision. The external carotid artery (ECA) was also ligated. Ischemia was induced by advancing the tip of a rounded 3–0 nylon suture into the internal carotid artery through the ECA. After placement, the intraluminal suture was secured by tying it around the ECA (90 min). Reperfusion was produced by withdrawing the intraluminal suture. In the sham group, the ECA was surgically prepared for the insertion of the filament, but the filament was not inserted.

Measurement of infarct volume: Following MCAO surgery and 5 days of reperfusion, the rats were sacrificed via decapitation. The brains were cut into coronal slices (2 mm thickness) with the aid of a brain matrix. The coronal brain slices were immediately immersed into 2% 2,3,5,-triphenyltetrazolium chloride (TTC; Sigma) for 10 min at 37 °C, following which they were fixed in 4% paraformaldehyde (PFA) solution (Prolabo, Paris, France) overnight before analysis. Brain slices were scanned individually, and the unstained area was analyzed using an image analysis system (Adobe Systems Inc., San Jose, CA). The areas of MCAO-induced ipsilateral cerebral infarction were determined based on loss of TTC staining. Areas of infarction were traced and analyzed using Image J software (NIH), version 1.32.

Experimental procedure for KIOM-2015EE application: The rats were randomly divided into eight groups (15 rats in each group)—sham-operated control, MCAO+PBS vehicle, MCAO-KIOM-2015EE 1 mg/ml or 2 mg/ml for eye drops, KIOM-2015EE 100 mg/kg or 200 mg/kg for oral administration or eye drops, KIOM-2015EW 2 mg/ml for eye drop, and positive drug 20 mg/kg (Ginexin-F Tab, 80 mg, SK Chemical, Gyeonggi-do, Korea) for oral administration. Retinal damage was induced by MCAO operation in all rats, with the exception of the sham-operated control group. Beginning the day after MCAO ischemic injury, the right eye of each rat in the experimental groups was treated three times daily (09:00, 15:00, 21:00) with topical drops or once daily with the oral formula. On day 5, all rats were sacrificed. Eye tissues were carefully harvested for histological analysis after the following preparations.

Retinal flat mount: Flat mounting was performed in accordance with previously described methods [31]. All rats were euthanized, following which their eyes were harvested. Harvested eyes were rinsed in PBS and then fixed in 4% PFA for 15 min. Eyes were transferred into a Petri dish, and the lens, sclera, and choroid were removed. The cup-shaped retina was transferred to the plate, and four to five radial incisions were made. Methanol was added dropwise to the surface of the retina until complete coverage was achieved. When the retina turned white, it was placed in methanol for at least 20 min. Fixed retinas were maintained in methanol at −20 °C until staining.

Paraffin embedding and histological examination: The collected eyeballs were fixed in 4% PFA in PBS for 24 h at 4 °C, following which they were washed twice in PBS. The samples were then dehydrated through an ethanol series, cleared by soaking in xylene, embedded in paraffin, and sectioned into 3-µm slices using a microtome (RM 2125RT; Leica Microsystems, Wetzlar, Germany). Slides containing paraffin sections were deparaffinized in xylene and rehydrated through an ethanol series. Hematoxylin and eosin (H&E) staining was then performed for histopathological examination. The specimens were mounted with Permount (Fisher, Fair Lawn, NJ), and images were captured using a Nikon fluorescence microscope equipped with NIS-Elements BR 4.50 software (Nikon, Tokyo, Japan).

Immunofluorescence staining of flat-mounted retinas: For immunofluorescence staining, the retinal tissues were removed from methanol, washed three times for 30 min each time in PBS, and transferred to glass slides. The specimens were permeabilized and blocked with 0.3% Triton-X/0.2% BSA (BSA)/5% normal goat serum in Tris-buffered saline (TBS; Perm/Block solution) for 1 h at 4 °C. The specimens were then incubated overnight with monoclonal antibodies against Tuj-1 or Brn3a and polyclonal antibodies against GFAP (diluted 1:50–100) in Perm/Block solution. Specimens were then washed three times in TBS, following which they were further incubated with the appropriate Alexa488- or 555- conjugated secondary antibodies at room temperature for 1 h. Specimens were again washed three times in PBS and stained with DAPI (Vectashield mounting medium).

Imaging the whole-mount retina for cell counts: Images were captured using a Nikon fluorescence microscope equipped with NIS-Elements BR 4.50 software (Nikon). Images from each retina were captured from an area located 100 µm from the optic nerve disc. For each condition, we randomly selected five images from among the captured photos and automatically measured the number of ganglion cells (Brn3a-positive cells) using ImageJ software. Total ganglion cell numbers were calculated as the average of three out of five measured results, excluding the minimum and maximum values.

Immunofluorescence staining of vertical retinal sections: For immunofluorescence staining, sectioned retinal tissue slides were deparaffinized in xylene in a 65 °C incubator for 1 h, following which they were rehydrated through an ethanol series. The specimens were permeabilized with 0.3% Triton™ X-100 for 10 min and blocked overnight with 5% normal goat serum and BSA in TBS at 4 °C. The specimens were then incubated overnight with monoclonal or polyclonal antibodies against glutamine synthetase, PKCα, parvalbumin, and recoverin (diluted 1:50–100) in 5% BSA. They were then washed three times in TBS, further incubated with the appropriate Alexa Fluor® 555-conjugated secondary antibodies at room temperature for 1 h, washed again three times with PBS, and stained with DAPI (Vectashield mounting medium). Images were captured using a Nikon fluorescence microscope equipped with NIS-Elements BR 4.50 software (Nikon). Red-positive cells were viewed at excitation and emission

wavelengths of 543 nm and 633 nm, respectively. The density of red fluorescence was measured using the Color Histogram function of the ImageJ software program.

TUNEL assay: The specimens were subjected to a terminal deoxynucleotidyl transferase (TdT) dUTP nick-end labeling (TUNEL) assay using an in situ cell death detection kit and fluorescein (Roche Diagnostics, Cat. No. 11 684 795 910), in accordance with the manufacturer's instructions. The positive-control sample was incubated with DNase I (3000 U/mL in 50 mM Tris/HCl), and the negative-control sample was incubated with label solution only. TUNEL-positive cells were viewed using a Nikon fluorescence microscope equipped with NIS-Elements BR 4.50 software (Nikon). The total number of cells and number of TUNEL-positive cells were counted in five individual high-power fields in each of the five samples. All slides were read by an experienced scientist who was blinded to the evaluation, and the scores and average ratio of the number of TUNEL-positive cells to the total number of cells were calculated.

High-performance liquid chromatography (HPLC) analysis: The KIOM-2015EW and KIOM-2015EE were extracted in 100% methanol (10 mg/ml) via ultrasound for 30 min. Standard compounds including orientin, isoorientin, and vitexin were dissolved in 100% methanol (1 mg/mL). All working solutions were filtered through a 0.2-mm syringe membrane filter (Whatman Ltd., Maidstone, UK) before injection into the HPLC system.

The analytical HPLC data were obtained using a Dionex Ultimate 3000 system equipped with a binary pump, autosampler, column oven, and diode array ultraviolet–visible spectroscopy (UV/VIS) detector (DAD). The output signal of the detector was recorded using the Chromeleon software of the HPLC system. Chromatographic separation was achieved on a Xbridge® C_{18} column (5 µm, 4.6 × 250 mm, Waters Co., Milford, MA) using trifluoroacetic acid (TFA) water (0.1%, v/v); solvent A, and acetonitrile. Solvent B was used as a mobile phase at a flow rate of 1 mL/min. The injection volume of each sample was 5 µL, and the column temperature was maintained at 40 °C. Briefly, the mobile phase consisted of water containing (A) 0.1% TFA and (B) acetonitrile with gradient elution at a flow rate of 1 mL/min. The HPLC elution condition was optimized as follows: 0–3 min, 5% B; 3–5 min, 5%–10% B; 5–15 min, 10%–15% B; 15–35 min, 15%–22% B; and 35–55 min, 22%–45% B. Identification of the peaks was based on the spectrum and retention time of each marker component from the KIOM-2015EW and KIOM-2015EE extracts.

Statistical analysis: Data were evaluated using one-way analyses of variance, followed by a Tukey's test. The analyses were performed using GraphPad PRISM software® (GraphPad PRISM software Inc., Version 5.02, San Diego, CA). The results are expressed as the mean ± standard error of the mean (SEM), and the level of statistical significance was set at $p<0.05$.

RESULTS

Animal models of MCAO-induced retinal ischemia injury: Five days after MCAO, we examined tissue infarction in the ipsilateral hemisphere of the experimental rats. As shown in Figure 1A, infarct volume in the MCAO model group was significantly higher than that in the sham-operated group. Infarct volumes in the MCAO model group significantly differed from those in the sham-operated control group (0.86±0.13% and 31.55±1.162%; $p<0.001$, respectively; Figure 1A).

KIOM-2015E promotes RGC survival following MCAO-induced retinal ischemia injury: Five days after MCAO-induced retinal ischemia injury, flat-mounted retinal tissues were stained with the RGC marker anti-Brn3a, and the captured photos were analyzed to determine the number of cells (Figure 1B).

MCAO-induced retinal ischemia injury resulted in an approximately 36.24% loss of RGCs (remaining RGC 63.80%±9.07; $p<0.001$). The application of KIOM-2015E after MCAO injury resulted in a significant protective effect against RGC loss (MCAO+KIOM-2015EE 100 mg/kg, oral administration: 82.42%±4.72, $p<0.05$; MCAO+KIOM-2015EE 200 mg/kg, oral administration: 92.78%±3.83, $p<0.001$). As shown in Figure 2B, topical eye drops containing KIOM-2015E were associated with a slight increase in cell number after MCAO injury, although this difference was not significant. In contrast, oral administration of KIOM-2015E markedly increased RGC protection in a dose-dependent manner, suggesting that oral administration of KIOM-2015EE was more effective than topical administration.

KIOM-2015EE prevents degradation of RGC nerve fibers in MCAO injury: We also investigated whether KIOM-2015E inhibits RGC nerve fiber degradation via whole-mount immunohistochemical staining using the β-III tubulin (Tuj-1) antibody—a marker for RGCs and neurons—in rats with MCAO-induced retinal ischemia injury (Figure 1C). In the sham-operated control retina, Tuj-1-positive nerve fibers exhibited numerous branches with thick lines connecting the optic disc to the outer region of the retina. However, in the MCAO+PBS vehicle group, Tuj-1-positive nerve fibers underwent degenerative changes. The few remaining nerve fibers in the MCAO+PBS vehicle group were very weak and exhibited few connections in the optic disc region.

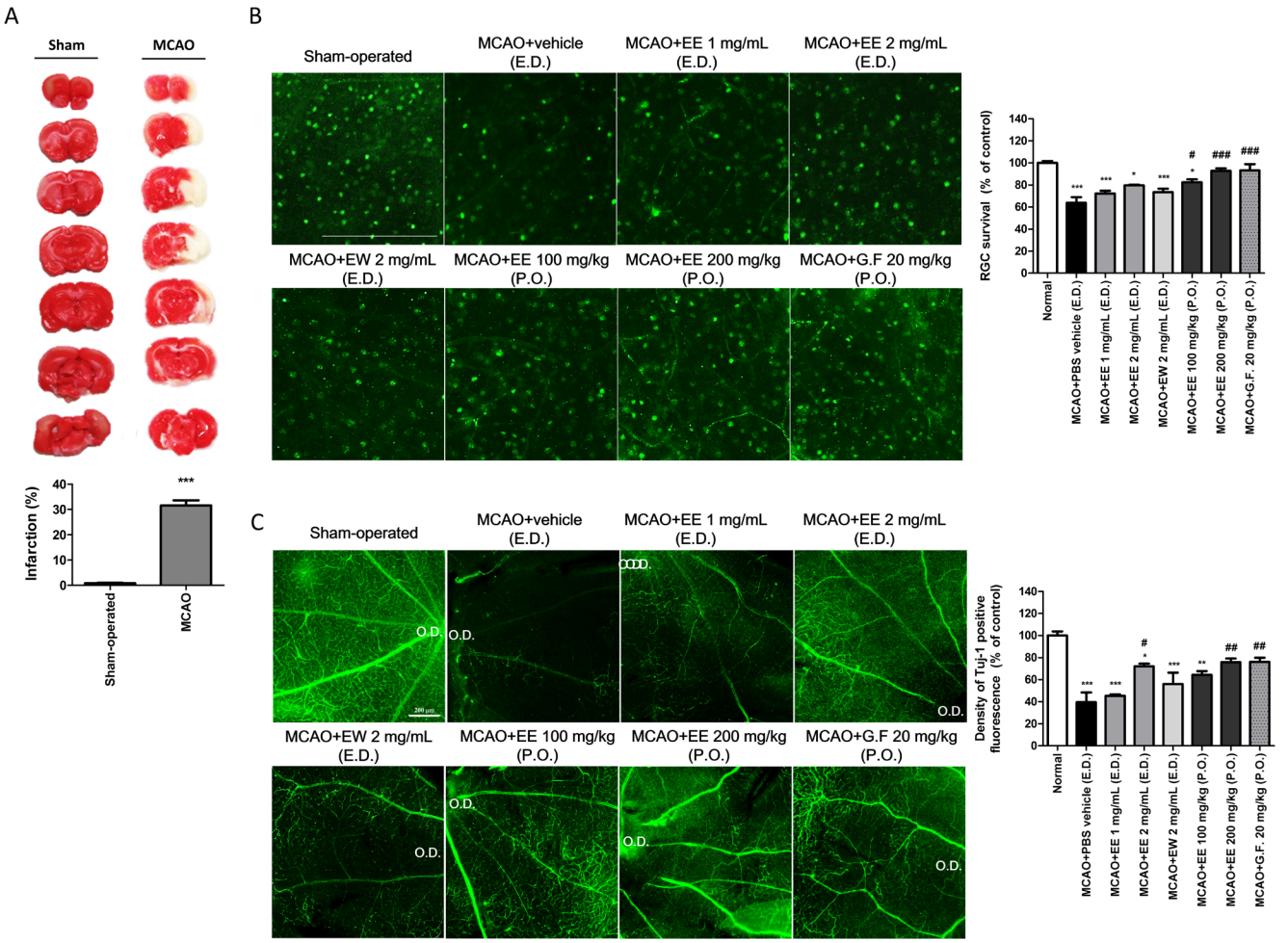

Figure 1. Application of KIOM-2015E for 5 days after MCAO decreased damage to RGCs and nerve fibers. **A**: Infarct volume as represented by TTC staining was used to indicate the degree of ischemic brain damage. Red staining indicates healthy tissue, as TTC does not stain areas of infarction. Relative to the sham-operated group, MCAO operation significantly increased infarct volume, which was quantified using the ImageJ program and represented as a percentage of the total brain volume. Data are presented as the mean ± standard error of the mean (SEM) from five individual rats in each group (n=5). ***p<0.001 versus the sham operated group. **B**: SD rats were treated using topical eye drops (E.D., three times daily) or via oral administration (P.O., once daily) of KIOM-2015EW, KIOM-2015EE, or Ginexin-F. Five days after treatment, loss of RGCs was determined by immunofluorescent staining of retinal flat mounts with antibodies against Brn3a. Quantitative analysis of RGCs in Brn3a-stained flat-mounted retinal tissues. While the number of Brn3a-positive RGCs was significantly reduced in rats with MCAO-induced injury, KIOM-2015E application protected RGCs from MCAO injury, as indicated by Brn3a-positive staining. The graph shows the average number of cells from five randomly selected photographs for each group. **C**: SD rats underwent treatment with E.D. (three times daily) and P.O. (once daily) formulations of KIOM-2015EW, KIOM-2015EE, or Ginexin-F. Five days after treatment, degradation of RGC nerve fibers was determined by immunofluorescent staining of retinal flat mounts with antibodies against class III beta-tubulin (Tuj-1). In the MCAO+vehicle group, severe degradation of nerve fibers was observed relative to that observed in the sham-operated group. However, treatment with KIOM-2015E inhibited the degradation of RGC nerve fibers. Quantitative analysis of fluorescence density was performed in Tuj-1 -stained flat-mounted retinal tissues. Five pictures were randomly selected per group. The average fluorescence density was calculated using the ImageJ program and expressed as a percentage of the value observed in the sham-operated group. All images were acquired at 40× magnification. Scale bar: 200 µm. Data are presented as means ± SEM *** p<0.001 versus sham-operated, # p<0.05, ## p<0.01, ###p<0.001 versus MCAO+vehicle (E.D.). TTC, 2,3,5-triphenyltetrazolium chloride; Brn3a, brain-specific homeobox/POU domain protein 3A; MCAO, middle cerebral artery occlusion; RGC, retinal ganglion cell; G.F., Ginexin F.

The density of Tuj-1-positive expression in this group had decreased to 39.48%±15.28 of that observed in sham-operated controls ($p<0.001$). In contrast, Tuj-1 protein expression was significantly upregulated in the MCAO+KIOM-2015E group. As shown in Figure 1C, the high-dose eye drops containing KIOM-2015E (MCAO+KIOM-2015EE 2 mg/ml: 72.06%±4.11, $p<0.05$) were associated with a greater degree of neuroprotection than low-dose eye drops containing KIOM-2015E (MCAO+KIOM-2015EE 1 mg/ml: 45.31%±2.20, $p<0.05$), and ethanol extracts (MCAO+KIOM-2015EE 2 mg/ml) had more neuroprotective effects than hot-water extracts (MCAO+KIOM-2015EW 2mg/ml: 56.06%±17.70)

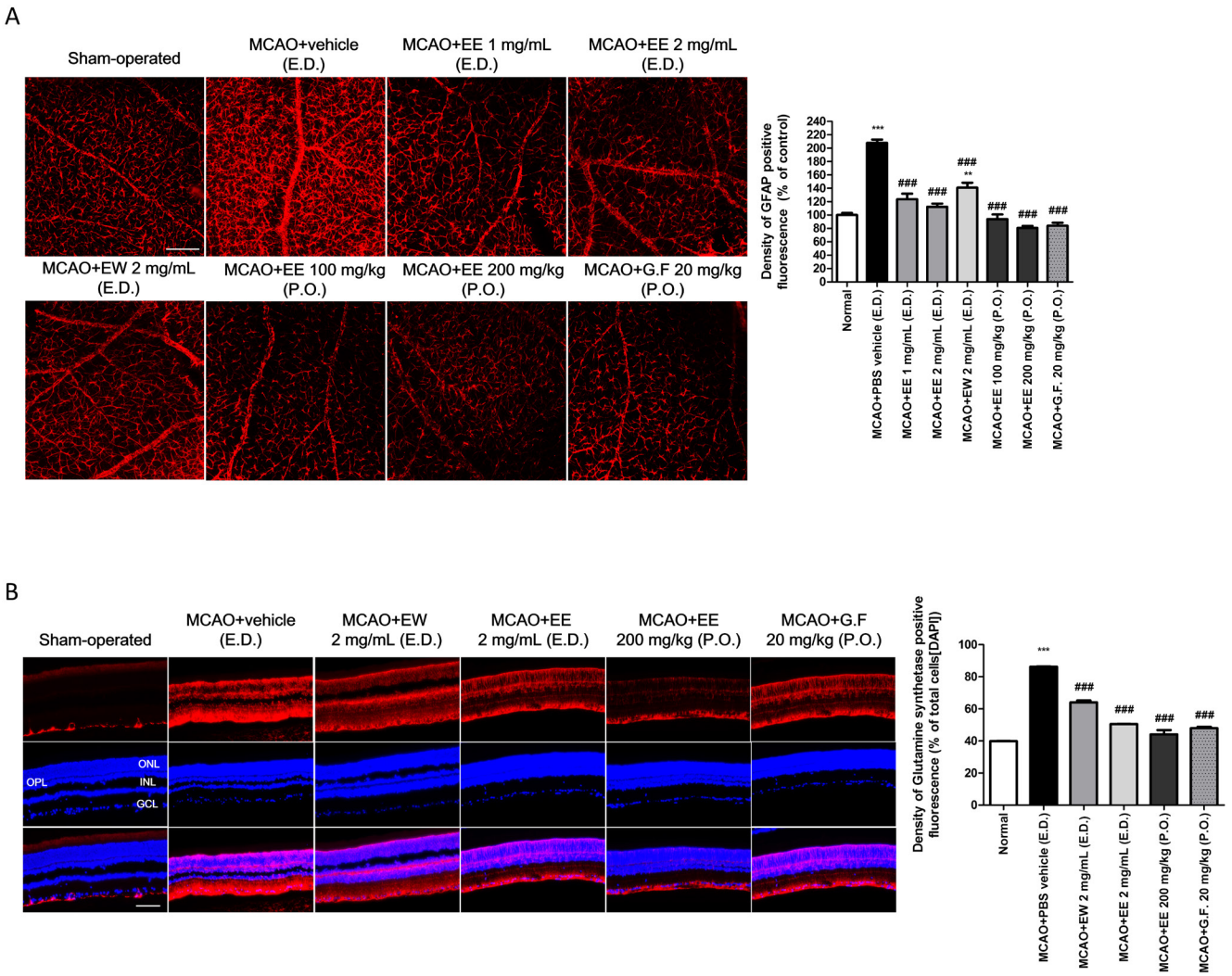

Figure 2. The application of KIOM-2015E for 5 days after MCAO inhibits the activation of Müller cells and astrocytes. SD rats were treated using topical eye drops (E.D., three times daily) or via oral administration (P.O., once daily) of KIOM-2015EW, KIOM-2015EE, or Ginexin-F. Five days after treatment, activation of Müller cells and astrocytes was determined by immunofluorescent staining of retinal flat mounts with antibodies against glial fibrillary acidic protein (GFAP; a marker of Müller and astrocytes; **A**) and by immunofluorescent staining of retinal tissue—which was paraffin-embedded and vertically sectioned—with an antibody against glutamine synthase (GS; a marker of astrocytes; **B**). Strong activation of GFAP and GS was observed in the MCAO+vehicle group relative to that observed in the sham-operated group. However, treatment with KIOM-2015E inhibited the activation of Müller cells and astrocytes. Quantitative analysis of fluorescence density in GFAP-stained flat-mounted and GS-stained vertically sectioned retinal tissues. Five pictures were randomly selected per group. The average fluorescence density was calculated using the ImageJ program and expressed as a percentage of the value for the sham-operated group. All images were acquired at 40× magnification. Scale bar: 200 μm. Data are presented as means ± standard error of the mean (SEM). ***p<0.001 versus sham-operated, ###p<0.001 versus MCAO+vehicle (E.D.). MCAO, middle cerebral artery occlusion; RGC, retinal ganglion cell; G.F., Ginexin F; GCL, ganglion cell layer.

at the same dose. Above all, oral administration of KIOM-2015E (MCAO+KIOM-2015EE 100 mg/kg: 64.35%±5.75; MCAO+KIOM-2015EE 200 mg/kg: 75.80%±5.76, p<0.01, respectively) exerted greater neuroprotective effects against damage due to retinal ischemia than the use of topical eye drops, and these effects were concentration-dependent. Taken together, our results suggest that KIOM-2015EE administration following MCAO injury has a neuroprotective function.

KIOM-2015E decreases GFAP expression in MCAO injury: Expression of GFAP serves as a marker of developmental processes and as an indicator of gliosis in response to injury [32]. GFAP is found in two glial cell types, astrocytes and Müller cells. We investigated whether KIOM-2015E regulates activation of GFAP in flat-mounted retinal tissue using immunoreactive staining for GFAP (Figure 2A). In the sham-operated control group, GFAP-positive fluorescence appeared uniformly scattered throughout the retina, although GFAP was expressed at low levels (100%±5.23). In contrast, GFAP-positive fluorescence was distinctly and strongly activated in rats with MCAO-induced retinal ischemic injury (207.90%±8.78, p<0.001). However, GFAP-positive fluorescence significantly decreased in all groups to which MCAO+KIOM-2015E was applied, relative to the MCAO injury group (MCAO+KIOM-2015EE 1 mg/ml: 123.77%±13.92, MCAO+KIOM-2015EE 2 mg/mL: 112.39%±8.30, MCAO+KIOM-2015EW 2 mg/ml: 140.91%±10.35, MCAO+KIOM-2015EE 100 mg/kg: 93.98%±11.97; MCAO+KIOM-2015EE 200 mg/kg: 80.70%±5.25, p<0.001, respectively). Both eye drops and oral administration decreased GFAP expression in a dose-dependent manner. Interestingly, in the case of eye drops, oral administration was more effective than eye drops.

KIOM-2015E promotes altered expression of GS after MCAO injury: GS immunostaining was used to indicate the location of Müller cells. As shown in Figure 2B, sham-operated retina tissue that had not been subjected to MCAO exhibited almost no GS-positive fluorescence, as only very small amounts of GS immunoreactivity were observed in the ganglion cell layer (GCL) and nerve fiber layer. In contrast, dramatic increases in GS-positive fluorescence expression were observed in retinal samples from rats with MCAO-induced retinal ischemic injury (86.29%±8.78, p<0.001), and GS-positive areas were detected in the ONL and subretinal space. In the GCL, GFAP expression, an indicator of retinal injury [33], was observed in parallel with a decrease in the number of ganglion cells. Our findings indicated that KIOM-2015E application markedly reduced GS-positive fluorescence expression (MCAO+KIOM-2015EW 2 mg/ml: 64.02%±1.64, MCAO+KIOM-2015EE 2 mg/ml: 50.53%±0.15, MCAO+KIOM-2015EE 200 mg/kg: 44.14%±3.77, p<0.001, respectively) and that oral administration was more effective than eye drops (Figure 2B). Both eye drops and oral administration were similar or more effective than the positive medication Ginexin F (47.96%±1.21, p<0.001).

Treatment with KIOM-2015E attenuates neuronal damage in the GCL and INL following MCAO injury: MCAO-induced ischemic retinal injury induced marked neuronal loss in the GCL of PBS-vehicle-treated animals (Figure 3A). The cells were loosely packed, and numerous empty spaces within the cellular layers were observed among the GCL, INL, and ONL. Quantitative analysis revealed there were fewer viable cells (63.10%±7.70, p<0.001) in PBS vehicle-treated animals with MCAO-induced retinal injury than in sham-operated controls (Figure 3A). However, treatment with KIOM-2015E appeared to overcome the loss of ganglion cells caused by MCAO injury, especially in the oral administration group (MCAO+KIOM-2015EE, 100 mg/kg: 86.31%±7.59; MCAO+KIOM-2015EE, 200 mg/kg: 88.10%±6.17, p<0.05, respectively). Although slight increases in the number of ganglion cells were observed in animals treated with eye drops, these differences were not statistically significant.

Apoptosis-induced neuronal damage in retinal tissue after MCAO-induced ischemic retinal injury was evaluated using TUNEL staining (Figure 3B). TUNEL staining in the sham-operated retina was negative (less than 10%±2.22), while TUNEL staining in the MCAO+PBS vehicle group was positive (33%±1.91; p<0.001), especially in the GCL and INL. However, KIOM-2015E treatment suppressed this apoptosis-induced neuronal damage following MCAO injury (MCAO+KIOM-2015EW 2 mg/mL: 17.13%±0.98, p<0.01; MCAO+KIOM-2015EE, 2 mg/ml: 14.63%±0.98; MCAO+KIOM-2015EE, 200 mg/kg: 11.65%±0.53, p<0.05, respectively).

Treatment with KIOM-2015E attenuates the loss of inner retinal neurons and histological changes in photoreceptor cells following MCAO injury: Changes in other cells of the retina were observed using specific antibodies to each, such as PKCα, parvalbumin, and recoverin as markers for bipolar cells, amacrine cells, and photoreceptors, respectively (Figure 4). The number of bipolar cells was significantly lower in the MCAO injury group than in the sham-operated control group (sham-operated: 55.0349±5.97%; MCAO+ PBS vehicle: 33.96±5.96, p<0.001, respectively). No obvious difference in the staining pattern for bipolar cells was noted between ischemic and KIOM-2015E-treated retinas (Figure 4A, upper panels; Figure 4B). Amacrine cells were labeled using anti-parvalbumin, and photoreceptor cells were labeled using anti-recoverin (Figure 4A, middle and lower panels). In the retina of sham-operated control rats, strong binding to the

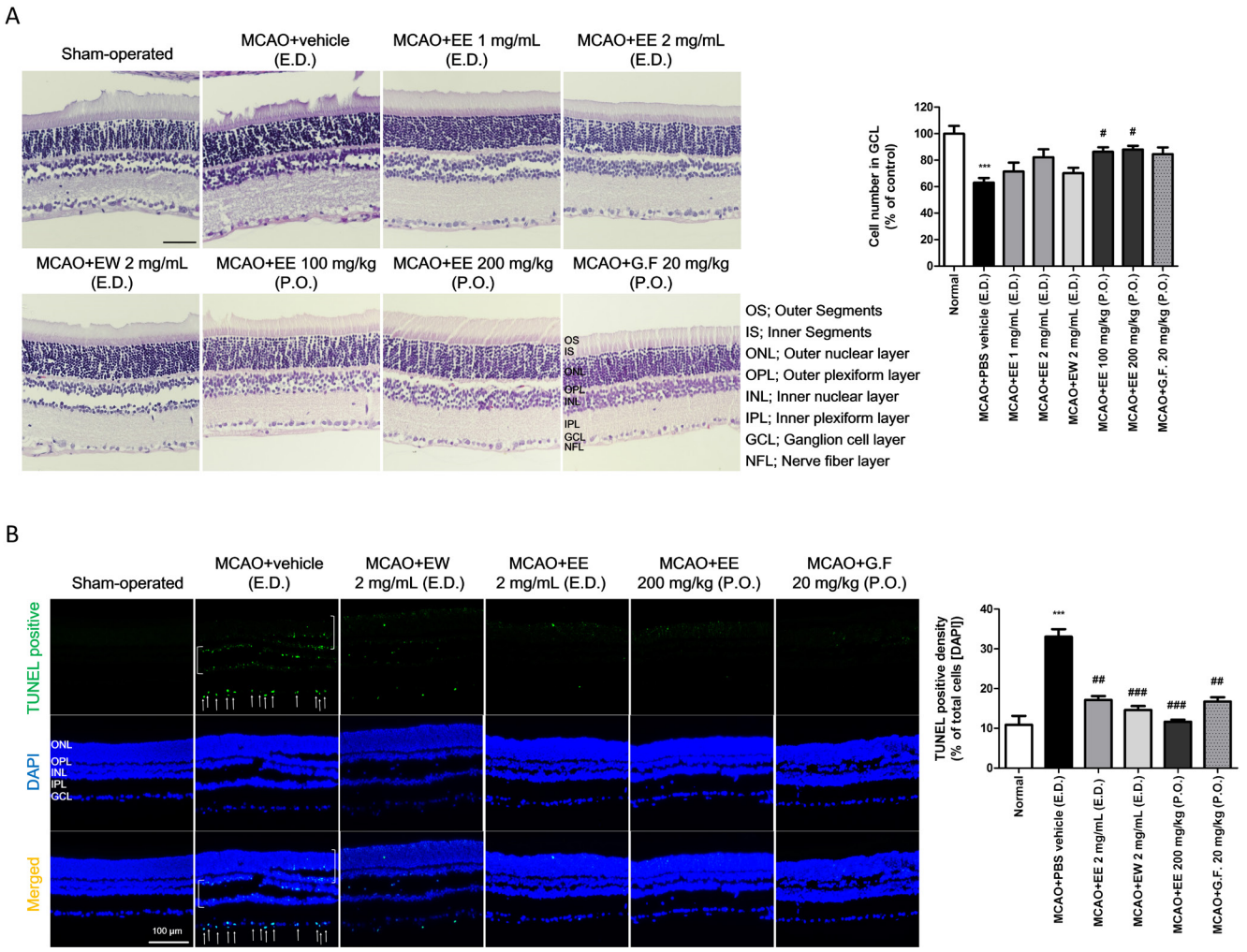

Figure 3. Protection against RGC and retinal tissue damage following treatment with KIOM-2015E. SD rats were treated using topical eye drops (E.D., thrice daily) or via oral administration (P.O., once daily) of KIOM-2015EW, KIOM-2015EE, or Ginexin-F. Five days after treatment, retinal tissues were analyzed via hematoxylin and eosin (H & E) staining and TUNEL assays after vertical sectioning. **A**: Significantly fewer RGCs were observed in the GCL of rats in the MCAO+vehicle group than in those of the sham-operated group. However, treatment with KIOM-2015E suppressed the loss of RGC. Quantitative analysis of RGC number in the GCL. Five pictures were randomly selected per group. The graph displays the average numbers of RGCs. **B**: Retinal sections were subjected to a TUNEL assay (green). Apoptotic RGCs were observed in the MCAO+vehicle group, while KIOM-2015E application reduced retinal tissue damage. Quantitative analysis of TUNEL-positive cells in the GCL. All images were acquired at 40× magnification. Scale bar: 100 µm. Data are presented as means ± standard error of the mean (SEM). ***p<0.001 versus sham-operated, # p<0.05, ## p<0.01, ### p<0.001 versus MCAO+vehicle (E.D.). MCAO, middle cerebral artery occlusion; RGC, retinal ganglion cell; G.F., Ginexin F; GCL, ganglion cell layer; TUNEL: terminal deoxynucleotidyl transferase dUTP nick-end labeling.

parvalbumin antibody was observed in a single row of cells on the inside of the INL and was detected in some cells of the GCL (26.16%±0.04). In addition, recoverin antibodies were detected in alignment with the ONL (72.33%±3.05). However, decreased anti-parvalbumin staining was observed in the INL and GCL (16.48±1.02, p<0.001), while decreased anti-recoverin staining was observed in the ONL of the MCAO + PBS vehicle group (60.86±1.15, p<0.001). In contrast, we observed increases in the number of amacrine (MCAO+KIOM-2015EW, 2 mg/mL: 27.51%±0.41; MCAO+KIOM-2015EE, 2 mg/mL: 27.52%±0.55; MCAO+KIOM-2015EE, 200 mg/kg: 27.20%±0.24, p<0.001, respectively) and photoreceptor cells (MCAO+KIOM-2015EW, 2 mg/mL: 65.14%±1.42; MCAO+KIOM-2015EE, 2 mg/mL: 70.58%±0.36; MCAO+KIOM-2015EE, 200 mg/kg: 71.02%±1.16, p<0.001, respectively) following the application of KIOM-2015EE. There was no significant difference between the two groups (Figure 4B), suggesting the

application of KIOM-2015EE protects inner retinal neurons from MCAO injury.

Identification of the main components in KIOM-2015EW and KIOM-2015EE using HPLC: According to the maximum absorption of the standards, the UV detector was set at 280 nm for HPLC analysis of orientin, isoorientin, and vitexin. The HPLC chromatograms of the standard mixture and KIOM-2015EW and KIOM-2015EE extract are presented in Figure 5. By comparing the retention times and UV spectral data with the standard compounds, peaks **1**, **2,** and **3** of KIOM-2015EW and KIOM-2015EE were identified as isoorientin, orientin, and vitexin, respectively. The mixed standards were indicated at retention times of 18.22 min (**1**), 19.21 min (**2**), and 22.38 min (**3**) in the chromatogram. Under the same conditions, the retention times of the observed components in KIOM-2015EW were 18.21 min (**1**), 19.21 min (**2**), and 22.45 min (**3**). These compounds were identified in the KIOM-2015EE at similar retention times (**1**, 18.22 min; **2**, 19.22 min; **3**, 22.45 min). Other major peaks could not be identified. Therefore, we are currently separating these peaks for nuclear magnetic resonance analysis.

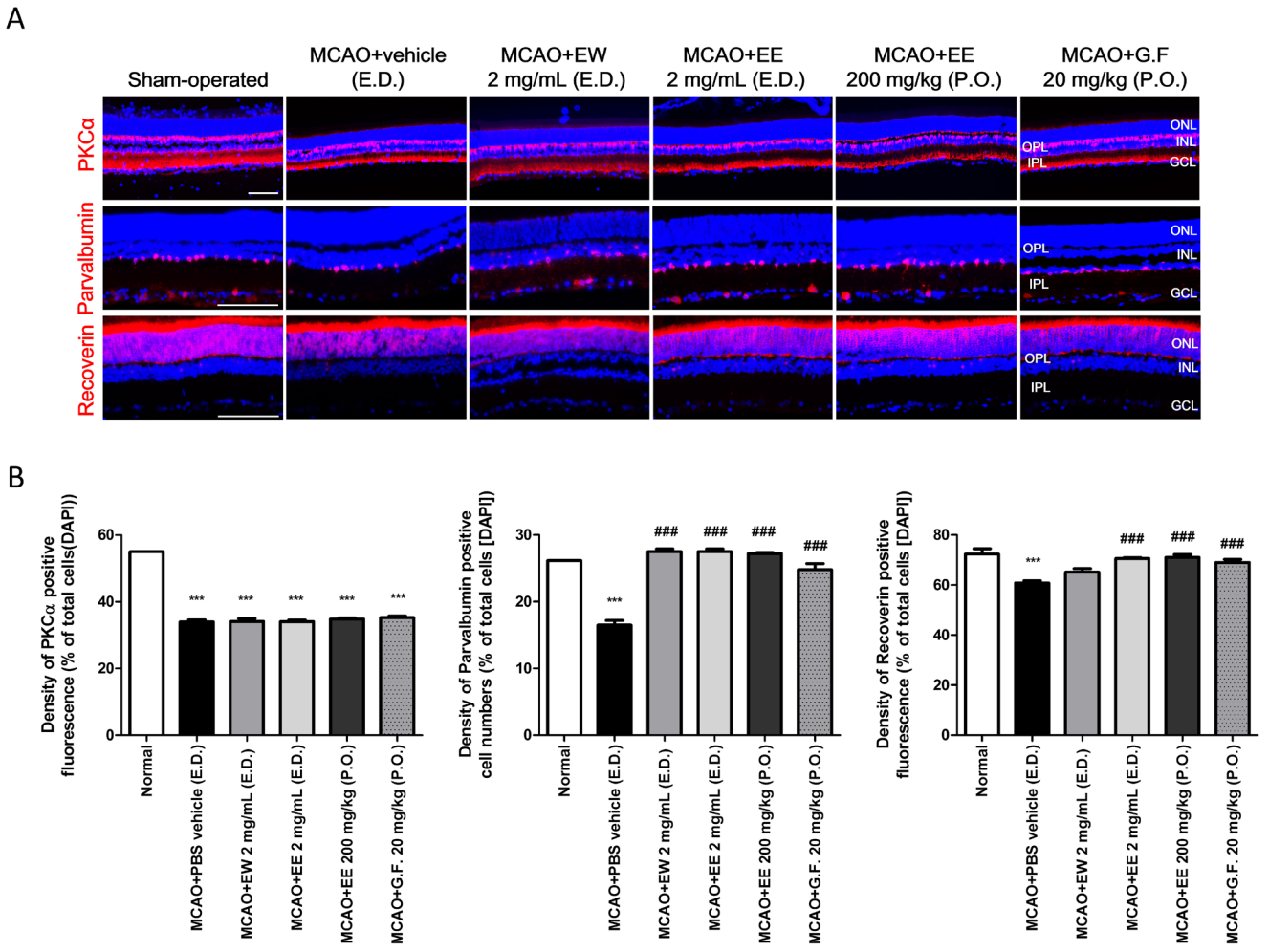

Figure 4. Immunohistochemistry for markers of inner retinal neurons. **A**: SD rats were treated using topical eye drops (E.D., three times daily) or via oral administration (P.O., once daily) of KIOM-2015EW, KIOM-2015EE, or Ginexin-F. Five days after treatment, sectioned retinal tissues underwent immunohistochemistry for the indicated markers (red) and were counterstained with DAPI (blue) after vertical sectioning. Protein kinase C alpha (PKCα), bipolar; parvalbumin, amacrine; recoverin, photoreceptors. **B**: Quantification of red fluorescence density was performed using the ImageJ software program. The figures depict the ratio of red fluorescence to DAPI fluorescence in the same region. All images were acquired at 40× magnification. Scale bar: 100 µm. Data are presented as mean ± standard error of the mean (SEM). ***p<0.001 versus sham-operated, ###p<0.001 versus MCAO+vehicle (E.D.). MCAO, middle cerebral artery occlusion; RGC, retinal ganglion cell; G.F., Ginexin F; GCL, ganglion cell layer.

DISCUSSION

In the present study, we investigated the neuroprotective effects of KIOM-2015E against MCAO-induced ischemic retinal injury in rats. As shown in Figure 1, these neuroprotective effects were more pronounced in animals treated via oral administration than in those treated with topical eye drops. Significant neuroprotective effects were observed on RGCs and their nerve fibers, cells of the inner retina, amacrine cells, and photoreceptor cells following treatment with eye drops containing high concentrations of the ethanol extract (Figure 1, Figure 3, and Figure 4) [34].

Retinal I/R is a pathophysiological process contributing to cellular damage in multiple ocular conditions, including glaucoma, diabetic retinopathy, and retinal vascular occlusions [35]. Following the induction of retinal ischemia, approximately 50% of RGCs die within the first 2 weeks after stroke [36]. Retinal ischemia is also a common cause of visual impairment and blindness [3]. Steele et al.. reported that MCAO is a sufficient method for inducing ischemic damage in the retina [19]. In our MCAO model, reperfusion was performed following 90 min of ischemic stress, which resulted in a 30% infarction in the brain after 5 days. Similarly, I/R injury produced a 36% loss of RGCs (Figure 1A, B), and Tuj-1 staining revealed that the level of nerve fiber expression had decreased to 39% of that observed in sham-operated control group (Figure 1C).

The MCAO procedure exerts similar damage on the brain and retinal tissues. As the retina is an extension of the diencephalon, retinal blood vessels share similar anatomic and physiologic properties with those in the brain and possess

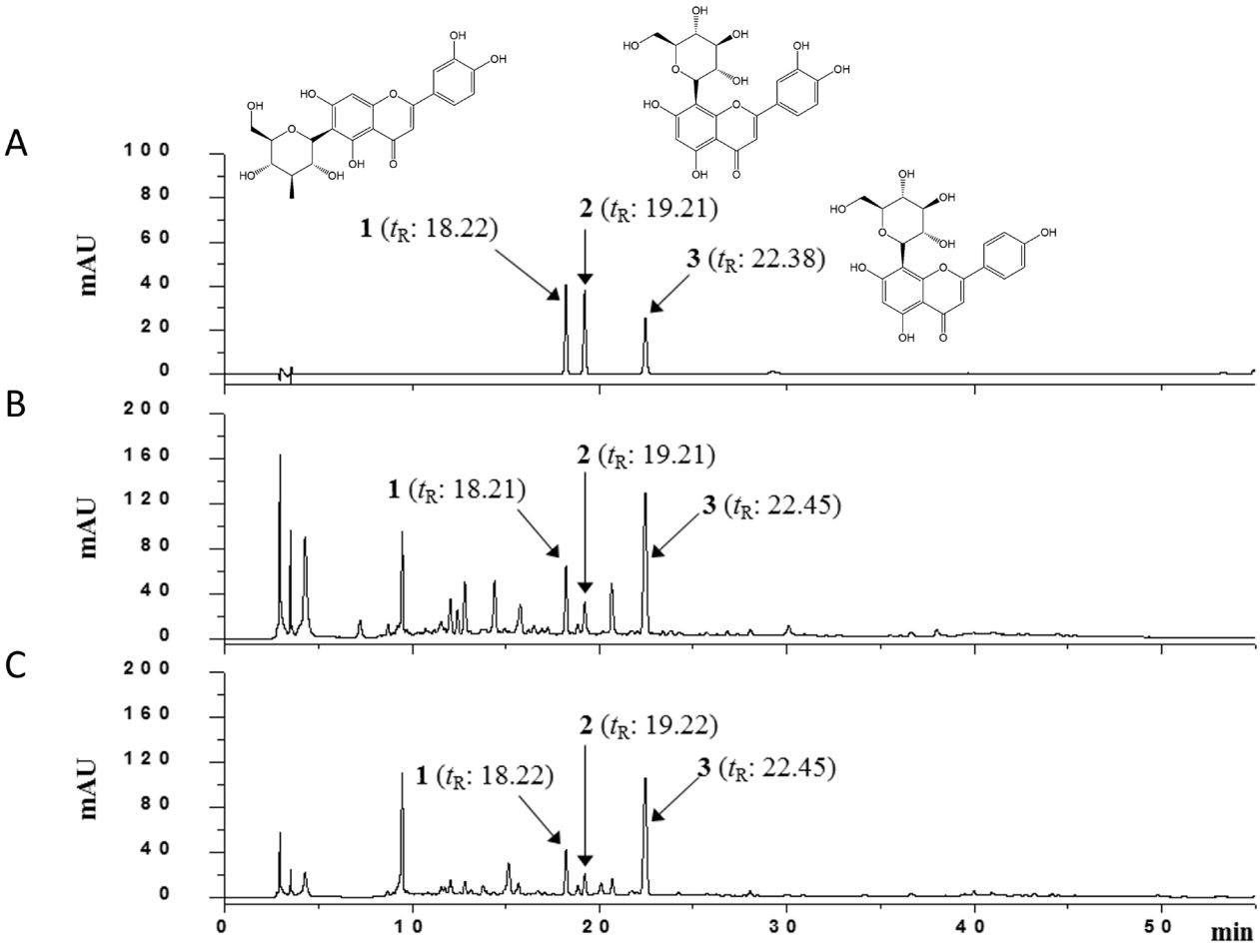

Figure 5. HPLC-DAD chromatograms of three compounds in KIOM-2015E. Isoorientin (**1**), orientin (**2**), vitexin (**3**) in standard mixture **(A);** KIOM-2015EW **(B);** and KIOM-2015EE **(C)** were identified at wavelengths of 280 nm. HPLC, high-performance liquid chromatography; DAD, diode array UV/VIS detector.

a blood-retinal barrier analogous to the blood–brain barrier [34].

There are two types of macroglial cells in the mammalian retina, astrocytes and Müller cells [37]. Astrocytes appear mainly in the optic nerve head and migrate to the nerve fiber layer and GCL [38]. They are restricted to the vitreous surface of the retina, where they are located largely within the nerve fiber layer [39]. In contrast, the Müller glial cells are specialized radial glial cells that extend from the inner limiting membrane to the outer liming membrane, providing functional and structural support to retinal neurons [40]. GFAP is an intermediate filament protein found in astrocytes and in Müller glial cell end-feet and processes. Although Müller glial cells in the normal rat retina express little or no GFAP [41], such cells exhibit increased GFAP expression in retinal injuries, including ischemia [42] and glaucoma [43]. In retinal diseases associated with I/R injury such as glaucoma, Müller cells and astrocytes display a hypertrophic morphology and an upregulation of GFAP [41,44]. Under normal conditions, Müller cells protect RGCs by releasing neurotrophic factors and secreting glutathione, which exerts antioxidant effects [40,44,45]. However, activated Müller cells negatively affect RGC survival in the ischemic retina [44,46,47]. GS is exclusively expressed in the soma of Müller glial cells [48]. These are the best reflections of altered glial reactivity [49,50].

To investigate changes in macroglial cell activity, we examined the expression of GFAP and GS in retinal sections obtained 5 days after MCAO injury (Figure 2A,B). As shown in Figure 2A, GFAP-positive staining was ubiquitously scattered throughout the flat-mounted retina, although the level of staining was low. However, following MCAO injury, GFAP expression significantly increased throughout the flat-mounted retina. Increased GFAP expression due to MCAO injury was reduced to almost normal levels following the application of KIOM-2015EE. In rats with MCAO injury, GS expression was also strongly increased throughout the layers of the vertically sectioned retinal tissue (Figure 2B). Macroglial activation is a key component of retinal neurodegeneration. Activation of two glial cell marker proteins by I/R injury was reduced by the application of KIOM-2015EE, which may have contributed to the preservation of retinal function. However, it is unknown whether MCAO-induced increases in GFAP and GS expression occurred immediately after surgery or gradually. Similarly, it remains unknown whether drug application produced effects on the first day or gradually. Therefore, future studies should compare the results of drug application among all 5 days. Nevertheless, our study demonstrates that the application of KIOM-2015EE reduces the activation of glial cells associated with I/R injury. Moreover, these effects were much more pronounced following oral administration than following the application of topical eye drops.

Recent advances in the field of neuroprotection indicate that healthy neurons can be protected from injury—and that damaged neurons can be rescued from death—by blocking specific steps in the cell death cascade [51]. Herbal products have been used in the treatment of various conditions, such as Parkinson's disease, coronary artery disease, cardiovascular disease, and traumatic injuries [52,53]. Romano et al. examined the neuroprotective activity of an extract from Chinese safflower (*Cartnamus tinchoris*, Honghua) [52,54]. Jung et al. demonstrated the in vitro antioxidant properties of *Thuja orientalis* extract in the transformed retinal ganglion cell line (RGC-5) [55]. The major component of this extract is isoquercitrin, which holds promise for the treatment of glaucoma but requires further study [52,55]. Matteucci et al. have also reported that curcumin, a phenolic extract obtained from *Curcuma longa*, exerted protective effects against NMDA excitotoxicity in both retinal and hippocampal neurons in primary retinal cell cultures [52,56]. Among the compounds identified in KIOM-2015EW and KIOM-2015EE, the major flavonoids were C-glycosyl flavones (orientin, isoorientin, and vitexin). Orientin, isoorientin, and vitexin are components of many natural plant extracts, and many other research groups have reported their anti-inflammatory [57-59], antioxidant [60,61], and neuroprotective effects [62-68]. Because these compounds are included in KIOM-2015EW and KIOM-2015EE, our findings support the notion that they exert neuroprotective effects in MCAO-induced retinal ischemia injury. Therefore, further studies will need to identify the neuroprotective effects of each of the above compounds.

In conclusion, the present study is the first to demonstrate the neuroprotective effect of KIOM-2015E on retinal cells following I/R and the regulation of macroglial cells in neurologic diseases. Taken together, our findings may aid in the development of novel therapeutic strategies against MCAO-induced retinal ischemia injury and other diseases associated with the degeneration of retinal cells, such as glaucoma, diabetic retinopathy, and age-related macular degeneration.

ACKNOWLEDGMENTS

This study was supported by Korea Institute of Oriental Medicine grants (K18101 and KSN1812101). We thank Young Jeung Park, director of Central Ophthalmic Clinic (Daegu, Korea) for advice on retinal disease.

REFERENCES

1. Goldblum D, Mittag T. Prospects for relevant glaucoma models with retinal ganglion cell damage in the rodent eye. Vision Res 2002; 42:471-8. [PMID: 11853763].
2. Colucciello M. Diabetic retinopathy. Control of systemic factors preserves vision. Postgrad Med 2004; 116:57-64. [PMID: 15274289].
3. Osborne NN, Chidlow G, Layton CJ, Wood JP, Casson RJ, Melena J. Optic nerve and neuroprotection strategies. Eye (Lond) 2004; 18:1075-84. [PMID: 15534592].
4. Hardy P, Beauchamp M, Sennlaub F, Gobeil F Jr, Tremblay L, Mwaikambo B, Lachapelle P, Chemtob S. New insights into the retinal circulation: inflammatory lipid mediators in ischemic retinopathy. Prostaglandins Leukot Essent Fatty Acids 2005; 72:301-25. [PMID: 15850712].
5. Bek T. Inner retinal ischaemia: current understanding and needs for further investigations. Acta Ophthalmol 2009; 87:362-7. [PMID: 19416114].
6. Rosenbaum DM, Degterev A, David J, Rosenbaum PS, Roth S, Grotta JC, Cuny GD, Yuan J, Savitz SI. Necroptosis, a novel form of caspase-independent cell death, contributes to neuronal damage in a retinal ischemia-reperfusion injury model. J Neurosci Res 2010; 88:1569-76. [PMID: 20025059].
7. Buchi ER. Cell death in the rat retina after a pressure-induced ischaemia-reperfusion insult: an electron microscopic study. I. Ganglion cell layer and inner nuclear layer. Exp Eye Res 1992; 55:605-13. [PMID: 1483506].
8. Piras A, Gianetto D, Conte D, Bosone A, Vercelli A. Activation of autophagy in a rat model of retinal ischemia following high intraocular pressure. PLoS One 2011; 6:e22514-[PMID: 21799881].
9. Selles-Navarro I, Villegas-Perez MP, Salvador-Silva M, Ruiz-Gomez JM, Vidal-Sanz M. Retinal ganglion cell death after different transient periods of pressure-induced ischemia and survival intervals. A quantitative in vivo study. Invest Ophthalmol Vis Sci 1996; 37:2002-14. [PMID: 8814140].
10. Cho JH, Mu X, Wang SW, Klein WH. Retinal ganglion cell death and optic nerve degeneration by genetic ablation in adult mice. Exp Eye Res 2009; 88:542-52. [PMID: 19109949].
11. Nakano N, Ikeda HO, Hangai M, Muraoka Y, Toda Y, Kakizuka A, Yoshimura N. Longitudinal and simultaneous imaging of retinal ganglion cells and inner retinal layers in a mouse model of glaucoma induced by N-methyl-D-aspartate. Invest Ophthalmol Vis Sci 2011; 52:8754-62. [PMID: 22003119].
12. Lam TT, Abler AS, Tso MO. Apoptosis and caspases after ischemia-reperfusion injury in rat retina. Invest Ophthalmol Vis Sci 1999; 40:967-75. [PMID: 10102294].
13. Junk AK, Mammis A, Savitz SI, Singh M, Roth S, Malhotra S, Rosenbaum PS, Cerami A, Brines M, Rosenbaum DM. Erythropoietin administration protects retinal neurons from acute ischemia-reperfusion injury. Proc Natl Acad Sci USA 2002; 99:10659-64. [PMID: 12130665].
14. Fontaine V, Mohand-Said S, Hanoteau N, Fuchs C, Pfizenmaier K, Eisel U. Neurodegenerative and neuroprotective effects of tumor Necrosis factor (TNF) in retinal ischemia: opposite roles of TNF receptor 1 and TNF receptor 2. J Neurosci 2002; 22:RC216-[PMID: 11917000].
15. Fukuda K, Hirooka K, Mizote M, Nakamura T, Itano T, Shiraga F. Neuroprotection against retinal ischemia-reperfusion injury by blocking the angiotensin II type 1 receptor. Invest Ophthalmol Vis Sci 2010; 51:3629-38. [PMID: 20164447].
16. Canazza A, Minati L, Boffano C, Parati E, Binks S. Experimental models of brain ischemia: a review of techniques, magnetic resonance imaging, and investigational cell-based therapies. Front Neurol 2014; 5:19-[PMID: 24600434].
17. Braeuninger S, Kleinschnitz C. Rodent models of focal cerebral ischemia: procedural pitfalls and translational problems. Exp Transl Stroke Med 2009; 1:8-[PMID: 20150986].
18. Ritzel RM, Pan SJ, Verma R, Wizeman J, Crapser J, Patel AR, Lieberman R, Mohan R, McCullough LD. Early retinal inflammatory biomarkers in the middle cerebral artery occlusion model of ischemic stroke. Mol Vis 2016; 22:575-88. [PMID: 27293375].
19. Steele EC Jr, Guo Q, Namura S. Filamentous middle cerebral artery occlusion causes ischemic damage to the retina in mice. Stroke 2008; 39:2099-104. [PMID: 18436885].
20. Smith RS. Systematic evaluation of the mouse eye: anatomy, pathology, and biomethods. Boca Raton: CRC Press; 2002.
21. Muthaian R, Minhas G, Anand A. Pathophysiology of stroke and stroke-induced retinal ischemia: emerging role of stem cells. J Cell Physiol 2012; 227:1269-79. [PMID: 21989824].
22. Niwa M, Aoki H, Hirata A, Tomita H, Green PG, Hara A. Retinal Cell Degeneration in Animal Models. Int J Mol Sci 2016; 17:110-25. [PMID: 26784179].
23. Block F, Grommes C, Kosinski C, Schmidt W, Schwarz M. Retinal ischemia induced by the intraluminal suture method in rats. Neurosci Lett 1997; 232:45-8. [PMID: 9292888].
24. Kaja S, Yang SH, Wei J, Fujitani K, Liu R, Brun-Zinkernagel AM, Simpkins JW, Inokuchi K, Koulen P. Estrogen protects the inner retina from apoptosis and ischemia-induced loss of Vesl-1L/Homer 1c immunoreactive synaptic connections. Invest Ophthalmol Vis Sci 2003; 44:3155-62. [PMID: 12824266].
25. Bi W, Gao Y, Shen J, He C, Liu H, Peng Y, Zhang C, Xiao P. Traditional uses, phytochemistry, and pharmacology of the genus Acer (maple): A review. J Ethnopharmacol 2016; 189:31-60. [PMID: 27132717].
26. Perkins TD, van den Berg AK. Maple syrup-production, composition, chemistry, and sensory characteristics. Adv Food Nutr Res 2009; 56:101-43. [PMID: 19389608].
27. Legault J, Girard-Lalancette K, Grenon C, Dussault C, Pichette A. Antioxidant activity, inhibition of nitric oxide overproduction, and in vitro antiproliferative effect of maple sap and syrup from Acer saccharum. J Med Food 2010; 13:460-8. [PMID: 20132041].

28. Gonzalez-Sarrias A, Li L, Seeram NP. Effects of maple (Acer) plant part extracts on proliferation, apoptosis and cell cycle arrest of human tumorigenic and non-tumorigenic colon cells. Phytother Res 2012; 26:995-1002. [PMID: 22147441].

29. Arnason T, Hebda RJ, Johns T. Use of plants for food and medicine by Native Peoples of eastern Canada. Can J Bot 1981; 59:2189-325. .

30. Kim YH, Oh TW, Park E, Yim NH, Park KI, Cho WK, Ma JY. Anti-Inflammatory and Anti-Apoptotic Effects of Acer Palmatum Thumb. Extract, KIOM-2015EW, in a Hyperosmolar-Stress-Induced In Vitro Dry Eye Model. Nutrients 2018; 10:282-299. [PMID: 29495608].

31. Tual-Chalot S, Allinson KR, Fruttiger M, Arthur HM. Whole mount immunofluorescent staining of the neonatal mouse retina to investigate angiogenesis in vivo. J Vis Exp 2013; 77e50546-[PMID: 23892721].

32. Sarthy PV, Fu M, Huang J. Developmental expression of the glial fibrillary acidic protein (GFAP) gene in the mouse retina. Cell Mol Neurobiol 1991; 11:623-37. [PMID: 1723659].

33. Dyer MA, Cepko CL. p57(Kip2) regulates progenitor cell proliferation and amacrine interneuron development in the mouse retina. Development 2000; 127:3593-605. [PMID: 10903183].

34. Tso MO, Jampol LM. Pathophysiology of hypertensive retinopathy. Ophthalmology 1982; 89:1132-45. [PMID: 7155524].

35. Hartsock MJ, Cho H, Wu L, Chen WJ, Gong J, Duh EJ. A Mouse Model of Retinal Ischemia-Reperfusion Injury Through Elevation of Intraocular Pressure. J Vis Exp 2016; 113:e54065-[PMID: 27501124].

36. Lafuente MP, Villegas-Perez MP, Selles-Navarro I, Mayor-Torroglosa S, Miralles de Imperial J, Vidal-Sanz M. Retinal ganglion cell death after acute retinal ischemia is an ongoing process whose severity and duration depends on the duration of the insult. Neuroscience 2002; 109:157-68. [PMID: 11784707].

37. Bussow H. The astrocytes in the retina and optic nerve head of mammals: a special glia for the ganglion cell axons. Cell Tissue Res 1980; 206:367-78. [PMID: 6771013].

38. Norton WT, Aquino DA, Hozumi I, Chiu FC, Brosnan CF. Quantitative aspects of reactive gliosis: a review. Neurochem Res 1992; 17:877-85. [PMID: 1407275].

39. Ridet JL, Malhotra SK, Privat A, Gage FH. Reactive astrocytes: cellular and molecular cues to biological function. Trends Neurosci 1997; 20:570-7. [PMID: 9416670].

40. Newman E, Reichenbach A. The Muller cell: a functional element of the retina. Trends Neurosci 1996; 19:307-12. [PMID: 8843598].

41. Bignami A, Dahl D. The radial glia of Muller in the rat retina and their response to injury. An immunofluorescence study with antibodies to the glial fibrillary acidic (GFA) protein. Exp Eye Res 1979; 28:63-9. [PMID: 376324].

42. Larsen AK, Osborne NN. Involvement of adenosine in retinal ischemia. Studies on the rat. Invest Ophthalmol Vis Sci 1996; 37:2603-11. [PMID: 8977474].

43. Xue LP, Lu J, Cao Q, Hu S, Ding P, Ling EA. Muller glial cells express nestin coupled with glial fibrillary acidic protein in experimentally induced glaucoma in the rat retina. Neuroscience 2006; 139:723-32. [PMID: 16458441].

44. Bringmann A, Pannicke T, Grosche J, Francke M, Wiedemann P, Skatchkov SN, Osborne NN, Reichenbach A. Muller cells in the healthy and diseased retina. Prog Retin Eye Res 2006; 25:397-424. [PMID: 16839797].

45. Harada T, Harada C, Watanabe M, Inoue Y, Sakagawa T, Nakayama N, Sasaki S, Okuyama S, Watase K, Wada K, Tanaka K. Functions of the two glutamate transporters GLAST and GLT-1 in the retina. Proc Natl Acad Sci USA 1998; 95:4663-6. [PMID: 9539795].

46. Kobayashi M, Kuroiwa T, Shimokawa R, Okeda R, Tokoro T. Nitric oxide synthase expression in ischemic rat retinas. Jpn J Ophthalmol 2000; 44:235-44. [PMID: 10913641].

47. Bringmann A, Pannicke T, Biedermann B, Francke M, Iandiev I, Grosche J, Wiedemann P, Albrecht J, Reichenbach A. Role of retinal glial cells in neurotransmitter uptake and metabolism. Neurochem Int 2009; 54:143-60. [PMID: 19114072].

48. Riepe RE, Norenburg MD. Muller cell localisation of glutamine synthetase in rat retina. Nature 1977; 268:654-5. [PMID: 19708].

49. Lam TK, Chan WY, Kuang GB, Wei H, Shum AS, Yew DT. Differential expression of glial fibrillary acidic protein (GFAP) in the retinae and visual cortices of rats with experimental renal hypertension. Neurosci Lett 1995; 198:165-8. [PMID: 8552312].

50. Chen H, Weber AJ. Expression of glial fibrillary acidic protein and glutamine synthetase by Muller cells after optic nerve damage and intravitreal application of brain-derived neurotrophic factor. Glia 2002; 38:115-25. [PMID: 11948805].

51. Miller NR. Optic nerve protection, regeneration, and repair in the 21st century: LVIII Edward Jackson Memorial lecture. Am J Ophthalmol 2001; 132:811-8. [PMID: 11730643].

52. Minhas G, Anand A. Animal models of retinal ischemia. Brain Injury-Pathogenesis, Monitoring Recovery and Management: InTech. 2011; 8:153-74. .

53. More SV, Kumar H, Kang SM, Song SY, Lee K, Choi DK. Advances in neuroprotective ingredients of medicinal herbs by using cellular and animal models of Parkinson's disease. Evid Based Complement Alternat Med 2013; 2013:957875-[PMID: 24073012].

54. Romano C, Price M, Bai H, Olney J. Neuroprotectants in Honghua: glucose attenuates retinal ischemic damage. Invest Ophthalmol Vis Sci 1993; 34:72-80. [PMID: 8425843].

55. Jung SH, Kim BJ, Lee EH, Osborne NN. Isoquercitrin is the most effective antioxidant in the plant Thuja orientalis and able to counteract oxidative-induced damage to a transformed cell line (RGC-5 cells). Neurochem Int 2010; 57:713-21. [PMID: 20708054].

56. Matteucci A, Cammarota R, Paradisi S, Varano M, Balduzzi M, Leo L, Bellenchi GC, De Nuccio C, Carnovale-Scalzo G, Scorcia G, Frank C, Mallozzi C, Di Stasi AM, Visentin S, Malchiodi-Albedi F. Curcumin protects against NMDA-induced toxicity: a possible role for NR2A subunit. Invest Ophthalmol Vis Sci 2011; 52:1070-7. [PMID: 20861489].

57. Seo CS, Lee MY, Shin IS, Lee JA, Ha H, Shin HK. Spirodela polyrhiza (L.) Sch. ethanolic extract inhibits LPS-induced inflammation in RAW264.7 cells. Immunopharmacol Immunotoxicol 2012; 34:794-802. [PMID: 22303922].

58. Nam TG, Lim TG, Lee BH, Lim S, Kang H, Eom SH, Yoo M, Jang HW, Kim DO. Comparison of Anti-Inflammatory Effects of Flavonoid-Rich Common and Tartary Buckwheat Sprout Extracts in Lipopolysaccharide-Stimulated RAW 264.7 and Peritoneal Macrophages. Oxid Med Cell Longev 2017; 2017:9658030-[PMID: 28928906].

59. Gou KJ, Zeng R, Dong Y, Hu QQ, Hu HW, Maffucci KG, Dou QL, Yang QB, Qin XH, Qu Y. Anti-inflammatory and Analgesic Effects of Polygonum orientale L. Extracts. Front Pharmacol 2017; 8:562-[PMID: 28912714].

60. Flores G, Dastmalchi K, Dabo AJ, Whalen K, Pedraza-Penalosa P, Foronjy RF, D'Armiento JM, Kennelly EJ. Antioxidants of therapeutic relevance in COPD from the neotropical blueberry Anthopterus wardii. Food Chem 2012; 131:119-25. [PMID: 22363097].

61. Clouzeau C, Godefroy D, Riancho L, Rostène W, Baudouin C, Brignole-Baudouin F. Hyperosmolarity potentiates toxic effects of benzalkonium chloride on conjunctival epithelial cells in vitro. Mol Vis 2012; 18:851-[PMID: 22529703].

62. Tian T, Zeng J, Zhao G, Zhao W, Gao S, Liu L. Neuroprotective effects of orientin on oxygen-glucose deprivation/reperfusion-induced cell injury in primary culture of rat cortical neurons. Exp Biol Med 2018; 2018:1535370217737983-[PMID: 29073777].

63. Na CS, Lee MJ, Hong SS, Choi Y-H, Lee J-E, Park S-Y, Lee YH, Hong SH. Antioxidant and Neuroprotective Activity of the Aerial Parts of Seven Eragrostis Species and Bioactive Compounds from E. japonica. Rec Nat Prod 2017; 12:101-6. .

64. Yuan L, Wu Y, Ren X, Liu Q, Wang J, Liu X. Isoorientin attenuates lipopolysaccharide-induced pro-inflammatory responses through down-regulation of ROS-related MAPK/NF-κB signaling pathway in BV-2 microglia. Mol Cell Biochem 2014; 386:153-65. [PMID: 24114663].

65. Law BNT, Ling APK, Koh RY, Chye SM, Wong YP. Neuroprotective effects of orientin on hydrogen peroxide-induced apoptosis in SH-SY5Y cells. Mol Med Rep 2014; 9:947-54. [PMID: 24366367].

66. Jung S, Lee H, Kim K-A, Lee E, Kim C, Um B. Identification of Radical Scavenging Compound From the Leaves of Phyllostachys nigra by Online HPLC-ABTS+ and Its Neuroprotective Effects Against Oxidative Stress in Retinal Ganglion Cells. Invest Ophthalmol Vis Sci 2010; 51:4742-.

67. Venuprasad M, Kumar KH, Khanum F. Neuroprotective effects of hydroalcoholic extract of Ocimum sanctum against H2O2 induced neuronal cell damage in SH-SY5Y cells via its antioxidative defence mechanism. Neurochem Res 2013; 38:2190-200. [PMID: 23996399].

68. Zhou X, Gan P, Hao L, Tao L, Jia J, Gao B, Liu JY, Zheng LT, Zhen X. Antiinflammatory effects of orientin-2"-O-galactopyranoside on lipopolysaccharide-stimulated microglia. Biol Pharm Bull 2014; 37:1282-94. [PMID: 25087950].

Articles are provided courtesy of Emory University and the Zhongshan Ophthalmic Center, Sun Yat-sen University, P.R. China. The print version of this article was created on 10 October 2020. This reflects all typographical corrections and errata to the article through that date. Details of any changes may be found in the online version of the article.